$K*(892)^0$ production in relativistic heavy ion collisions at $\sqrt{s_{NN}}=130$ GeV

C. Adler,[11] Z. Ahammed,[23] C. Allgower,[12] J. Amonett,[14] B. D. Anderson,[14] M. Anderson,[5] G. S. Averichev,[9] J. Balewski,[12] O. Barannikova,[9,23] L. S. Barnby,[14] J. Baudot,[13] S. Bekele,[20] V. V. Belaga,[9] R. Bellwied,[31] J. Berger,[11] H. Bichsel,[30] A. Billmeier,[31] L. C. Bland,[2] C. O. Blyth,[3] B. E. Bonner,[24] A. Boucham,[26] A. Brandin,[18] A. Bravar,[2] R. V. Cadman,[1] H. Caines,[33] M. Calderón de la Barca Sánchez,[2] A. Cardenas,[23] J. Carroll,[15] J. Castillo,[26] M. Castro,[31] D. Cebra,[5] P. Chaloupka,[20] S. Chattopadhyay,[31] Y. Chen,[6] S. P. Chernenko,[9] M. Cherney,[8] A. Chikanian,[33] B. Choi,[28] W. Christie,[2] J. P. Coffin,[13] T. M. Cormier,[31] J. G. Cramer,[30] H. J. Crawford,[4] A. A. Derevschikov,[22] L. Didenko,[2] T. Dietel,[11] J. E. Draper,[5] V. B. Dunin,[9] J. C. Dunlop,[33] V. Eckardt,[16] L. G. Efimov,[9] V. Emelianov,[18] J. Engelage,[4] G. Eppley,[24] B. Erazmus,[26] P. Fachini,[2] V. Faine,[2] J. Faivre,[13] R. Fatemi,[12] K. Filimonov,[15] E. Finch,[33] Y. Fisyak,[2] D. Flierl,[11] K. J. Foley,[2] J. Fu,[15,32] C. A. Gagliardi,[27] N. Gagunashvili,[9] J. Gans,[33] L. Gaudichet,[26] M. Germain,[13] F. Geurts,[24] V. Ghazikhanian,[6] O. Grachov,[31] V. Grigoriev,[18] M. Guedon,[13] E. Gushin,[18] T. J. Hallman,[2] D. Hardtke,[15] J. W. Harris,[33] T. W. Henry,[27] S. Heppelmann,[21] T. Herston,[23] B. Hippolyte,[13] A. Hirsch,[23] E. Hjort,[15] G. W. Hoffmann,[28] M. Horsley,[33] H. Z. Huang,[6] T. J. Humanic,[20] G. Igo,[6] A. Ishihara,[28] Yu. I. Ivanshin,[10] P. Jacobs,[15] W. W. Jacobs,[12] M. Janik,[29] I. Johnson,[15] P. G. Jones,[3] E. G. Judd,[4] M. Kaneta,[15] M. Kaplan,[7] D. Keane,[14] J. Kiryluk,[6] A. Kisiel,[29] J. Klay,[15] S. R. Klein,[15] A. Klyachko,[12] T. Kollegger,[11] A. S. Konstantinov,[22] M. Kopytine,[14] L. Kotchenda,[18] A. D. Kovalenko,[9] M. Kramer,[19] P. Kravtsov,[18] K. Krueger,[1] C. Kuhn,[13] A. I. Kulikov,[9] G. J. Kunde,[33] C. L. Kunz,[7] R. Kh. Kutuev,[10] A. A. Kuznetsov,[9] L. Lakehal-Ayat,[26] M. A. C. Lamont,[3] J. M. Landgraf,[2] S. Lange,[11] C. P. Lansdell,[28] B. Lasiuk,[33] F. Laue,[2] J. Lauret,[2] A. Lebedev,[2] R. Lednický,[9] V. M. Leontiev,[22] M. J. LeVine,[2] Q. Li,[31] S. J. Lindenbaum,[19] M. A. Lisa,[20] F. Liu,[32] L. Liu,[32] Z. Liu,[32] Q. J. Liu,[30] T. Ljubicic,[2] W. J. Llope,[24] G. LoCurto,[16] H. Long,[6] R. S. Longacre,[2] M. Lopez-Noriega,[20] W. A. Love,[2] T. Ludlam,[2] D. Lynn,[2] J. Ma,[6] R. Majka,[33] S. Margetis,[14] C. Markert,[33] L. Martin,[26] J. Marx,[15] H. S. Matis,[15] Yu. A. Matulenko,[22] T. S. McShane,[8] F. Meissner,[15] Yu. Melnick,[22] A. Meschanin,[22] M. Messer,[2] M. L. Miller,[33] Z. Milosevich,[7] N. G. Minaev,[22] J. Mitchell,[24] C. F. Moore,[28] V. Morozov,[15] M. M. de Moura,[31] M. G. Munhoz,[25] J. M. Nelson,[3] P. Nevski,[2] V. A. Nikitin,[10] L. V. Nogach,[22] B. Norman,[14] S. B. Nurushev,[22] G. Odyniec,[15] A. Ogawa,[21] V. Okorokov,[18] M. Oldenburg,[16] D. Olson,[15] G. Paic,[20] S. U. Pandey,[31] Y. Panebratsev,[9] S. Y. Panitkin,[2] A. I. Pavlinov,[31] T. Pawlak,[29] V. Perevoztchikov,[2] W. Peryt,[29] V. A. Petrov,[10] M. Planinic,[12] J. Pluta,[29] N. Porile,[23] J. Porter,[2] A. M. Poskanzer,[15] E. Potrebenikova,[9] D. Prindle,[30] C. Pruneau,[31] J. Putschke,[16] G. Rai,[15] G. Rakness,[12] O. Ravel,[26] R. L. Ray,[28] S. V. Razin,[9,12] D. Reichhold,[8] J. G. Reid,[30] G. Renault,[26] F. Retiere,[15] A. Ridiger,[18] H. G. Ritter,[15] J. B. Roberts,[24] O. V. Rogachevski,[9] J. L. Romero,[5] A. Rose,[31] C. Roy,[26] V. Rykov,[31] I. Sakrejda,[15] S. Salur,[33] J. Sandweiss,[33] I. Savin,[10] J. Schambach,[28] R. P. Scharenberg,[23] N. Schmitz,[16] L. S. Schroeder,[15] A. Schüttauf,[16] K. Schweda,[15] J. Seger,[8] D. Seliverstov,[18] P. Seyboth,[16] E. Shahaliev,[9] K. E. Shestermanov,[22] S. S. Shimanskii,[9] G. Skoro,[9] N. Smirnov,[33] R. Snellings,[15] P. Sorensen,[6] J. Sowinski,[12] H. M. Spinka,[1] B. Srivastava,[23] E. J. Stephenson,[12] R. Stock,[11] A. Stolpovsky,[31] M. Strikhanov,[18] B. Stringfellow,[23] C. Struck,[11] A. A. P. Suaide,[31] E. Sugarbaker,[20] C. Suire,[2] M. Šumbera,[20] B. Surrow,[2] T. J. M. Symons,[15] A. Szanto de Toledo,[25] P. Szarwas,[29] A. Tai,[6] J. Takahashi,[25] A. H. Tang,[15] D. Thein,[6] J. H. Thomas,[15] M. Thompson,[3] V. Tikhomirov,[18] M. Tokarev,[9] M. B. Tonjes,[17] T. A. Trainor,[30] S. Trentalange,[6] R. E. Tribble,[27] V. Trofimov,[18] O. Tsai,[6] T. Ullrich,[2] D. G. Underwood,[1] G. Van Buren,[2] A. M. VanderMolen,[17] I. M. Vasilevski,[10] A. N. Vasiliev,[22] S. E. Vigdor,[12] S. A. Voloshin,[31] F. Wang,[23] H. Ward,[28] J. W. Watson,[14] R. Wells,[20] G. D. Westfall,[17] C. Whitten ,Jr.,[6] H. Wieman,[15] R. Willson,[20] S. W. Wissink,[12] R. Witt,[33] J. Wood,[6] N. Xu,[15] Z. Xu,[2] A. E. Yakutin,[22] E. Yamamoto,[15] J. Yang,[6] P. Yepes,[24] V. I. Yurevich,[9] Y. V. Zanevski,[9] I. Zborovský,[9] H. Zhang,[33] W. M. Zhang,[14] R. Zoulkarneev,[10] and A. N. Zubarev[9]

(STAR Collaboration)

[1]*Argonne National Laboratory, Argonne, Illinois 60439*
[2]*Brookhaven National Laboratory, Upton, New York 11973*
[3]*University of Birmingham, Birmingham, United Kingdom*
[4]*University of California, Berkeley, California 94720*
[5]*University of California, Davis, California 95616*
[6]*University of California, Los Angeles, California 90095*
[7]*Carnegie Mellon University, Pittsburgh, Pennsylvania 15213*
[8]*Creighton University, Omaha, Nebraska 68178*
[9]*Laboratory for High Energy (JINR), Dubna, Russia*
[10]*Particle Physics Laboratory (JINR), Dubna, Russia*
[11]*University of Frankfurt, Frankfurt, Germany*
[12]*Indiana University, Bloomington, Indiana 47408*
[13]*Institut de Recherches Subatomiques, Strasbourg, France*
[14]*Kent State University, Kent, Ohio 44242*
[15]*Lawrence Berkeley National Laboratory, Berkeley, California 94720*

[16]*Max-Planck-Institut für Physik, Munich, Germany*
[17]*Michigan State University, East Lansing, Michigan 48824*
[18]*Moscow Engineering Physics Institute, Moscow, Russia*
[19]*City College of New York, New York City, New York 10031*
[20]*Ohio State University, Columbus, Ohio 43210*
[21]*Pennsylvania State University, University Park, Pennsylvania 16802*
[22]*Institute of High Energy Physics, Protvino, Russia*
[23]*Purdue University, West Lafayette, Indiana 47907*
[24]*Rice University, Houston, Texas 77251*
[25]*Universidade de Sao Paulo, Sao Paulo, Brazil*
[26]*SUBATECH, Nantes, France*
[27]*Texas A&M, College Station, Texas 77843*
[28]*University of Texas, Austin, Texas 78712*
[29]*Warsaw University of Technology, Warsaw, Poland*
[30]*University of Washington, Seattle, Washington 98195*
[31]*Wayne State University, Detroit, Michigan 48201*
[32]*Institute of Particle Physics, Wuhan, Hubei 430079, China*
[33]*Yale University, New Haven, Connecticut 06520*
(Received 22 May 2002; published 30 December 2002)

We report the first observation of $K^*(892)^0 \rightarrow \pi K$ in relativistic heavy ion collisions. The transverse momentum spectrum of $(K^{*0} + \bar{K}^{*0})/2$ from central Au+Au collisions at $\sqrt{s_{NN}} = 130$ GeV is presented. The ratios of the K^{*0} yield derived from these data to the yields of negative hadrons, charged kaons, and ϕ mesons have been measured in central and minimum bias collisions and compared with model predictions and comparable e^+e^-, pp, and $\bar{p}p$ results. The data indicate no dramatic reduction of K^{*0} production in relativistic heavy ion collisions despite expected losses due to rescattering effects.

Modification of meson resonance production rates and their in-medium properties are among the proposed signals of a possible phase transition of nuclear matter to a deconfined plasma of quarks and gluons in relativistic heavy ion collisions [1]. For resonances like K^{*0} with a lifetime comparable to the time scale for evolution of the dense matter created in such collisions, characteristic properties such as width, branching ratio, yield, and transverse momentum spectra are expected to be sensitive to the dynamics and chiral properties of the high energy density medium which is produced [1,2].

More generally, the study of short-lived hadronic resonances as a means to utilize the extended spectrum of hadronic matter to probe hadron production under extreme conditions also provides important insight into the relative probability that a quark-antiquark pair will form a vector resonance meson as compared to a pseudoscalar partner [3]. This relates directly to the role of spin in hadron production in strongly interacting matter under extreme conditions. Additionally, the study of higher level resonances affords a better understanding of feed-down to stable particles from resonance decays [4] to further constrain thermal models of particle production [5–7] in nucleus-nucleus collisions.

Resonances which decay into strongly interacting hadrons in the dense matter are less likely to be reconstructed due to rescattering of the daughter particles. Resonances with higher p_T have a larger probability of decaying outside the system and therefore of being detected. Alternatively, the resonance yield could be increased during the rescattering phase between chemical freeze-out (vanishing inelastic collisions) and kinetic freeze-out (vanishing elastic collisions)

[8–10] via elastic processes like $\pi K \rightarrow K^{*0} \rightarrow \pi K$. This regeneration mechanism would partially compensate for resonance decays if the expansion of the produced matter took a relatively long time ($\gtrsim 20$ fm/c), increasing the observed ratio of K^{*0}/K. By systematically comparing the yields and transverse momentum distributions of resonances with other particles, it should be possible to distinguish different freeze-out conditions [11,12], such as sudden freeze-out or a slow expansion of the final state hadrons.

Another reason the study of the K^{*0} is interesting is its strange quark content. The enhancement of strangeness production in heavy ion collisions has long been predicted to be a signature of the formation of a deconfined quark-gluon plasma [13]. The combined measurement of the K^{*0} and ϕ mesons provides an additional, unique tool to distinguish various hadronic expansion and freeze-out scenarios [11,4,14].

The $K^*(892)^0$ and its antiparticle are the dominant resonances in the $K\pi$ system [15]. In previous relativistic heavy ion experiments the observation of these resonances has been problematic due to backgrounds from other $K\pi$ partial waves [16], decays of higher mass resonances [17], elliptic flow [18], and detector limitations (particle misidentification, acceptance, and efficiency, etc.). Due to the increased energy of the beams available at the Relativistic Heavy Ion Collider (RHIC), it was expected from simulation that the yield of these resonances would be sufficiently large for them to be observed using the mixed event method successfully used to reconstruct the ϕ meson at RHIC [19].

The detector system used for these studies was the Solenoidal Tracker at RHIC (STAR). The main tracking device
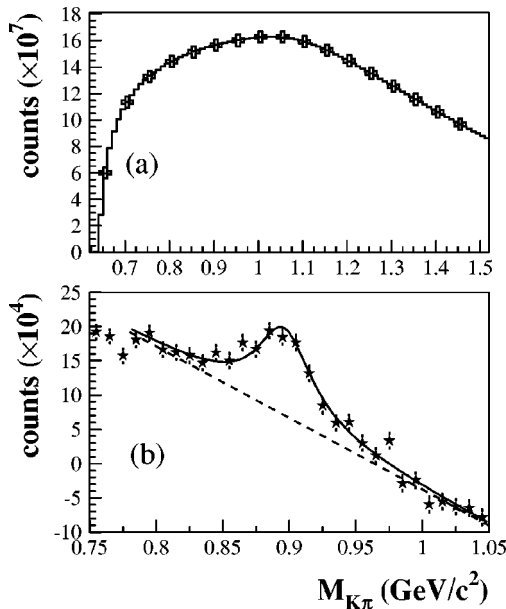
FIG. 1. (a) $K\pi$ invariant mass distribution from same-event pairs (symbols shown every 50 MeV) and mixed-event pairs (histogram) from central collisions for 0.4 GeV/$c < p_T < 2.8$ GeV/c. (b) $K*^0$ invariant mass distribution after subtraction of the mixed-event reference distribution. A Breit-Wigner functional form (solid curve) was fit to the peak assuming a linear background residual (dashed line). The mass and width of the resonances used for the fit were fixed from the particle data book [17]. The data points reflect a bin size on the x axis of 10 MeV per bin.

within STAR is the time projection chamber (TPC) [20] which is used to provide momentum information and particle identification for charged particles by measuring their ionization energy loss (dE/dx). A minimum bias trigger was defined using coincidences between two zero degree calorimeters which measured the spectator neutrons. A central trigger barrel constructed of scintillator paddles surrounding the TPC was used to select small impact parameter "central" collisions by selecting events with high charged particle multiplcity.

Data were taken for Au+Au collisions at $\sqrt{s_{NN}}$ $= 130$ GeV. To achieve uniform acceptance in the pseudorapidity range studied [21], the collision vertex was required to be within ± 95 cm of the midpoint of the TPC along the beam direction. Approximately 440 000 central and 230 000 minimum bias events were used in this analysis. Particles were selected based on their momenta (p), track quality, and particle identification from the TPC dE/dx. Since the daughters of $K*^0$ decays originate at the interaction point, tracks were selected whose distance of closest approach to the primary interaction vertex was less than 3.0 cm. Charged kaons were selected by requiring their dE/dx to be within two standard deviations (2σ) of the expected mean. A looser dE/dx cut of 3σ was used for pions. Kaons and pions were required to have transverse momenta (p_T) between 0.2 and 2 GeV/c to enhance track quality [21]. In addition, the daughters were required to have pseudorapidities $|\eta| < 0.8$ with an opening angle of > 0.2 rad between them.
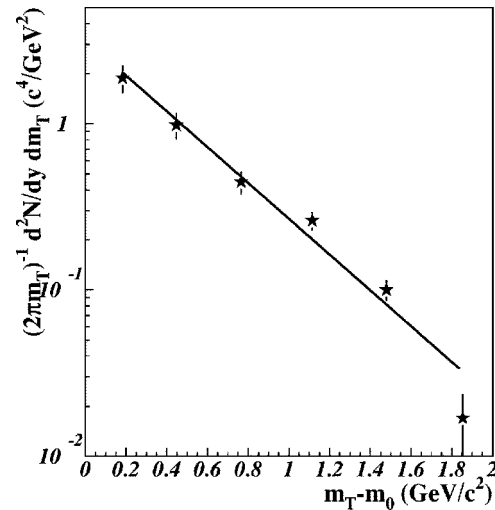

FIG. 2. The transverse mass m_T spectrum of $(K*^0 + \bar{K}*^0)/2$ within $|y| < 0.5$ for the 14% most central Au+Au interactions was studied. $K*^0$ resonances having 0.4 GeV/$c < p_T < 2.8$ GeV/c were detected. Error bars are statistical only.

The decay channels $K*^0 \rightarrow \pi^- K^+$ and $\bar{K}*^0 \rightarrow \pi^+ K^-$, both of which have a branching ratio of 2/3, were selected for the measurements. Due to limited statistics, it was necessary to combine these spectra. Therefore, the $K*^0$ yields presented in this Rapid Communication correspond to the average value of $K*^0$ and $\bar{K}*^0$ unless otherwise specified. To measure these yields, the invariant mass was calculated for each oppositely charged $K\pi$ pair in an event. The invariant mass distribution derived in this manner was then compared to a reference distribution calculated using uncorrelated kaons and pions from different events. Typically, three or more
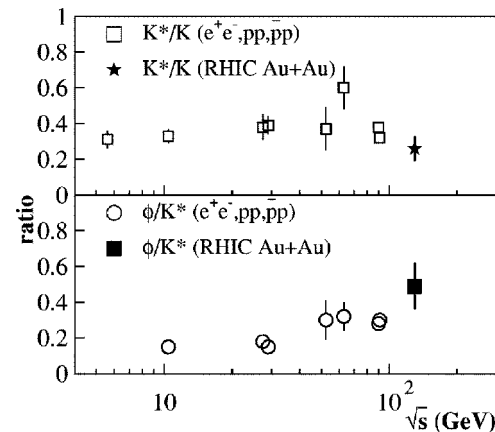

FIG. 3. The $K*^0$ to charged kaon and ϕ to $K*^0$ ratios for different colliding systems as a function of $\sqrt{s}$. Data are shown with quadratically combined systematical and statistical errors. The data are from collisions of $e^+ e^-$ at $\sqrt{s}$ of 10.45 GeV, 29 GeV, and 91 GeV [3,4,25,26], $\bar{p}p$ at 5.6 GeV [27], and pp from the ISR [22,28] at 63 and 52.5 GeV and NA27 [29] at 28 GeV. Ratios shown are for total integrated yields except for the present measurements ($|y| < 0.5$) and those from the ISR [22] at $\sqrt{s} = 63$ GeV where the ratio is for midrapidity.

events with similar multiplicity and collision vertex locations ($|\Delta Z| < 20$ cm) were used for this "mixed-event" technique.

From the 440 000 events in the 14% most central event data sample, more than 1.4×10^{10} oppositely charged kaon and pion pairs were analyzed. The corresponding invariant mass distribution is shown in Fig. 1(a) along with the mixed event reference distribution. The two distributions were normalized to each other at $M_{K\pi} \simeq 1$ GeV/c^2 which is close to the mass region of interest for this measurement. The two distributions are observed to match well; when subtracted the resulting distribution exhibits a K^{*0} signal which is ≈ 15 standard deviations above the background [Fig. 1(b)]. The signal to background ratio before background subtraction is about 1/1000 for central events and 1/200 for minimum bias Au+Au interactions. These ratios are significantly smaller than the value of 1/4 observed for proton-proton interactions at the CERN Intersecting Storage Rings (ISR) [22], indicating the increased difficulty of this measurement in the high multiplicity environment typical of relativistic nucleus-nucleus collisions.

As mentioned previously, higher mass resonant states in the $K\pi$ system as well as nonresonant $K\pi$ correlations also contribute to the same-event spectrum. In addition, particle misidentification of the decay products of the ρ, ω, η, and K_s^0 cause false correlations to appear in the same-event spectrum which are not present in the mixed-event spectrum used to estimate the background. Comparison of the real invariant mass distribution to a reference distribution derived using the HIJING [23] event generator suggests that the residual correlation near the K^{*0} mass peak may be due to the above sources. However, accurate determination of the magnitude of this residual correlation requires a detailed knowledge of the particle production and phase space distributions for the above particles, including those for the ρ and ω which are presently unmeasured. Several functional forms, including linear and exponential, were used to fit the residual background in Fig. 1(b). The choice of normalization for the mixed-event spectrum was also varied in order to study the stability of the resulting K^{*0} yield. The resulting differences in yield were within 20% in all cases, which was taken as a measure, in part, of the systematic uncertainty.

The uncorrected number of K^{*0} was calculated by integrating the Breit-Wigner function fit to the data assuming the linear residual background shown in Fig. 1(b). In order to determine the yield, detector acceptance and efficiency corrections were applied as well as a correction for the branching ratio. This was done by embedding simulated kaons and pions from $K^{*0}, \bar{K}^{*0}$ decays into real events using GEANT, and passing them through the full reconstruction chain [21]. The acceptance and efficiency factor ϵ depends on centrality, p_T, and the rapidity of the parent and daughter particles. It varied from about 10% for parent $p_T \simeq 0$ GeV/c to $\approx 35\%$ for parent $p_T \simeq 2.0$ GeV/c.

Figure 2 shows $d^2N/(2\pi m_T dm_T dy)$ as function of $m_T - m_0 = \sqrt{p_T^2 + m_0^2} - m_0$, where $m_0 = 0.896$ GeV/c^2 is the mass of the K^{*0} resonance [17]. An exponential fit was used to extract the K^{*0} yield per unit of rapidity around midrapidity, as well as the inverse slope (T). The fit yielded dN/dy

$= 10.0 \pm 0.9$ (stat) and $T = 0.40 \pm 0.02$ (stat) GeV for central collisions. The systematic uncertainty in dN/dy and T was estimated to be 25% and 10%, respectively, due to uncertainty in the tracking efficiency and in the determination of the background. Due to limited statistics, the inverse slope parameter derived for the central event sample was also used to extract dN/dy for the minimum bias sample. The result is 4.5 ± 0.7(stat)± 1.4(syst). The additional systematic error in this instance results from an estimate of the uncertainty in the inverse slope of the m_T spectrum. Combining all p_T bins, separate mass spectra of K^{*0} and $\bar{K}^{*0}$ were also fitted with a Breit-Wigner resonant function plus a linear residual background. The ratio of $\bar{K}^{*0}/K^{*0} = 0.92 \pm 0.14$ (stat) was obtained for central events. Consequently, the average of the combined K^{*0} and $\bar{K}^{*0}$ spectra should accurately represent $K^*(892)^0$ production within our statistics. This ratio is similar to K^-/K^+ ratio [24].

The K^{*0}/h^- ratio for the top 14% most central collisions is 0.042 ± 0.004(stat)± 0.01(syst) and 0.059 ± 0.008(stat) ± 0.019(syst) for minimum bias collisions where h^- is the total negative hadron yield with $|\eta| < 0.5$ [21]. These results can be compared with $K^{*0}/h^- = 0.036 \pm 0.002$ from e^+e^- collisions [4,17,25] at $\sqrt{s} = 91$ GeV and $K^{*0}/\pi^- = 0.057 \pm 0.009 \pm 0.009$ from pp collisions [22] at $\sqrt{s} = 63$ GeV. The ratio K^{*0}/h^- is observed to be approximately constant from low to high multiplicities at RHIC and is compatible with that measured in elementary particle collisions (e^+e^-, pp, and $\bar{p}p$).

With respect to studies of freeze-out conditions, the ratio K^{*0}/K is more interesting and less model dependent than K^{*0}/h^- since both particles have similar quark content and differ only in their spin and mass. By simple spin statistics, the vector meson to meson (pseudoscalar+vector) ratio would be 0.75. However, the measured ratio is much smaller in elementary collisions [4]. The charged kaon results used here are an average of K^+ and K^- in the same centrality range from Ref. [24]. The result, $K^{*0}/K = 0.26 \pm 0.03$(stat) ± 0.07(syst) in central Au+Au collisions at RHIC, can be compared with the average value of 0.37 ± 0.02 from e^+e^- [3,4,25,26], $\bar{p}p$ [27], and pp [22,28,29] as shown in Fig. 3.

In elementary collisions, the ϕ/K^{*0} ratio measures the strangeness suppression to good approximation since there is only a small mass difference between the ϕ and the K^{*0}, but the strangeness quantum number for these particles differs by one unit, strangeness being hidden in the ϕ meson. This ratio seems to increase in elementary particle collisions as a function of center-of-mass energy ($\sqrt{s}$). In this study, it was found that $\phi/K^{*0} = 0.49 \pm 0.05$(stat)$\pm 0.12$(syst) for the 14% most central collisions [19]. This result is greater than that from elementary collisions as shown in Fig. 3. The increased ratio at RHIC, compared to that in elementary processes, may be indicative of strangeness enhancement and/or additional effects (e.g., rescattering, coalescence [14]) on resonances in heavy ion collisions.

Since the lifetime of K^{*0} is comparable to the time scale for evolution of the Au+Au collision system, the K^{*0} survival probability must be accounted for when comparing the

results from Au+Au collisions with those from elementary particle collisions or with thermal model fits at chemical freeze-out. In general, the K^{*0} survival probability depends on the duration of the source (Δt), the size of the source for particle emission, and the p_T of the parent K^{*0}. If it is assumed that the difference between the K^{*0}/K ratio in heavy ion collisions and that observed in collisions of simpler systems is due to this survival probability alone, the indication would be that Δt ($\lesssim 4$ fm/c) is small. For large Δt ($\gtrsim 20$ fm/c) [12] without K^{*0} regeneration, the K^{*0} production should be an order of magnitude lower than the observed result [11], and the low p_T part of the transverse momentum distribution should be suppressed resulting in a larger effective inverse m_T slope. Although the measured K^{*0} inverse slope is larger than that of the charged kaons (most likely the result of radial flow [5,24]), it is still similar to that for the ϕ [$T=379\pm 50$(stat)± 45(syst) MeV] [19]. This is consistent with the interpretation of a short time (small Δt) between chemical and kinetic freeze-out.

Alternatively, elastic processes such as $\pi K \rightarrow K^{*0} \rightarrow \pi K$ are operative between chemical and kinetic freeze-out and partially regenerate the K^{*0} until kinetic freeze-out. In a statistical model description [5–7], the measured K^{*0} should reflect conditions at kinetic freeze-out rather than at chemical freeze-out if there is a long lived phase in which significant rescattering takes place. Within the framework of this type of model, reasonable values [5–7] of the chemical and kinetic freeze-out temperatures T_{ch} and T_{th}, pion chemical potentials μ_π at kinetic freeze-out [1,9], and the mass difference ($\Delta m = 0.4$ GeV) between K^{*0} and K can be obtained. These result in the ratio of $(K^{*0}/K)_{th}$ at kinetic freeze-out and $(K^{*0}/K)_{ch}$ at chemical freeze-out being roughly $(K^{*0}/K)_{th}/(K^{*0}/K)_{ch}=\exp[(-\Delta m+\mu_\pi)/T_{th}+\Delta m/T_{ch}]$ which is in the range of 0.3 to 1.2. The value measured in the present study (0.26) for kinetic freeze-out and the value of 0.37 assumed for chemical freeze-out are in the ratio of 0.7 ± 0.2, which selects specific trajectories in the phase diagram of μ_π/μ_B and T [9]. The ratio at chemical freeze-out is based on a statistical model [5–7], and upon collisions of lighter systems where the chemical and kinetic freeze-out processes are naturally overlapped.

Present measurements are not consistent with a long expansion time ($\Delta t \gtrsim 20$ fm/c) without significant K^{*0} regeneration. They are consistent with a sudden freeze-out interpretation ($\Delta t \lesssim 4$ fm/c). The simple estimates made in this paper illustrate how the study of resonance can provide important information on the dynamics and evolution of the matter produced in relativistic nucleus-nucleus collisions. More sophisticated analyses (e.g., comparison with transport models such as UrQMD [30]) with improved uncertainty in the measurement of the ϕ and K^{*0}, as well as the measurement of additional resonances are needed to determine the evolution of the system resulting from central heavy ion collisions in detail.

In conclusion, we have presented the first measurement of $K^*(892)^0$ and $\bar{K}^*(892)^0$ in relativistic nucleus-nucleus collisions. The K^{*0} m_T spectrum from the 14% most central Au+Au collisions results in an inverse slope parameter similar to that measured for the ϕ meson in similar centrality. The measured yield, $dN/dy=10.0\pm 0.9$(stat)± 2.5(syst) is relatively high compared to elementary collisions and thermal model predictions, considering the short K^{*0} lifetime ($c\tau \simeq 4$ fm) and expected losses due to rescattering of the decay daughters in the dense medium. The results of this study are consistent with two possible scenarios for the dynamic evolution of the system: (1) a short time duration between chemical and kinetic freeze-out (i.e., sudden freeze-out), or (2) a long period of expansion characterized by high hadron density and significant K^{*0} regeneration along specific trajectories in the phase diagram. Studies of strongly decaying resonant states like the K^{*0} open a new approach to the study of relativistic nucleus-nucleus collisions.

[1] R. Rapp and J. Wambach, Adv. Nucl. Phys. **25**, 1 (2000); R. Rapp, Phys. Rev. C **63**, 054907 (2001).

[2] J. Schaffner-Bielich, Phys. Rev. Lett. **84**, 3261 (2000).

[3] M. Derrick *et al.*, Phys. Lett. **158B**, 519 (1985).

[4] Y.J. Pei, Z. Phys. C **72**, 39 (1996), and references therein; P.V. Chliapnikov, Phys. Lett. B **470**, 263 (1999).

[5] N. Xu and M. Kaneta, Nucl. Phys. **A698**, 306c (2002).

[6] F. Becattini, Z. Phys. C **69**, 485 (1996); F. Becattini and U. Heinz, *ibid.* **76**, 269 (1997).

[7] P. Braun-Munzinger *et al.*, Phys. Lett. B **518**, 41 (2001).

[8] H. Bebie *et al.*, Nucl. Phys. **B378**, 95 (1992).

[9] R. Rapp and E.V. Shuryak, Phys. Rev. Lett. **86**, 2980 (2001); R. Rapp, Phys. Rev. C **66**, 017901 (2002).

[10] C. Song and V. Koch, Phys. Rev. C **55**, 3026 (1997).

[11] J. Letessier *et al.*, J. Phys. G **27**, 427 (2001); G. Torrieri and J. Rafelski, Phys. Lett. B **509**, 239 (2001); W. Broniowski and W. Florkowski, Phys. Rev. Lett. **87**, 272302 (2001).

[12] L.V. Bravina *et al.*, Phys. Rev. C **63**, 064902 (2001); D. Teaney *et al.*, nucl-th/0110037.

[13] J. Rafelski and B. Mueller, Phys. Rev. Lett. **48**, 1066 (1982); **56**, 2334(E) (1986).

[14] A.J. Baltz and C. Dover, Phys. Rev. C **53**, 362 (1996).

[15] M. Alston *et al.*, Phys. Rev. Lett. **6**, 300 (1961).

[16] M. Aguilar-Benitez *et al.*, Phys. Rev. D **6**, 11 (1972).

[17] Particle Data Group, D.E. Groom *et al.*, Eur. Phys. J. C **15**, 1 (2000).

[18] K.H. Ackermann *et al.*, Phys. Rev. Lett. **86**, 402 (2001).

[19] C. Adler *et al.*, Phys. Rev. C **65**, 041901(R) (2002).

[20] K.H. Ackermann *et al.*, Nucl. Phys. **A661**, 681 (1999).

[21] C. Adler *et al.*, Phys. Rev. Lett. **87**, 112303 (2001).

[22] T. Akesson *et al.*, Nucl. Phys. **B203**, 27 (1982).

[23] X.N. Wang and M. Gyulassy, Phys. Rev. D **44**, 3501 (1991); Comput. Phys. Commun. **83**, 307 (1994).

[24] C. Adler *et al.*, nucl-ex/0206008.

[25] K. Abe *et al.*, Phys. Rev. D **59**, 052001 (1999).

[26] H. Albrecht *et al.*, Z. Phys. C **61**, 1 (1994).

[27] J. Canter *et al.*, Phys. Rev. D **20**, 1029 (1979).

[28] D. Drijard *et al.*, Z. Phys. C **9**, 293 (1981).

[29] M. Aguilar-Benitez *et al.*, Z. Phys. C **50**, 405 (1991).

[30] M. Bleicher and J. Aichelin, Phys. Lett. B **530**, 81 (2002).